The influence of generalized gradient corrections to the LDA on predictions of structural phase stability: the Peierls distortion in As and Sb

1995 J. Phys.: Condens. Matter 7 3683

(http://iopscience.iop.org/0953-8984/7/19/002)

J. Phys.: Condens. Matter 7 (1995) 3683–3692. Printed in the UK

The influence of generalized gradient corrections to the LDA on predictions of structural phase stability: the Peierls distortion in As and Sb

K Seifert, J Hafner, J Furthmüller and G Kresse

Institut für Theoretische Physik, Technische Universität Wien, Wiedner Hauptstraße 8–10, A–1040 Wien, Austria

Received 17 January 1995

Abstract. The crystal structure and phase stability of the group-V elements As and Sb has been investigated by total-energy calculations within the local-density approximation (LDA), without and including generalized gradient corrections (GGC). We show that, contrary to the case of the group-VI elements Se and Te, where the LDA predicts crystal structures with a much smaller difference between the short intra-chain bonds and the long inter-chain bonds than is observed, for As and Sb the LDA leads to equilibrium structures in reasonable, or even good, agreement with experiment and describes the pressure-induced phase transition to a simple cubic structure in Sb (but not in As) very well. The GGC corrections show a tendency to overshoot and do not improve agreement with experiment. In both cases the main effect of the GGC is to add an isotropic pressure to the system, while the local electronic and bonding properties at constant volume remain unchanged.

1. Introduction

In recent years there has been considerable interest in developing techniques that allow one to overcome the well known limitations of the local density approximation (LDA) to the density functional theory [1,2] of the interacting many-electron system. Foremost among these limitations is the tendency of the LDA to overestimate the cohesive energy, the equilibrium density and the bulk modulus [2–4]. Generalized gradient corrections [5–7] to the LDA exchange-correlation functional represent an attempt to cure the deficiencies of the approach by incorporating lowest-order gradient corrections, while respecting the known sum rules for the exchange hole [8,9]. It has been shown that in some cases the GGC improve the energetics of s, p-bonded metals and semiconductors [10–12] with respect to the LDA, but there is certainly a tendency to overcorrect. For transition metals a general tendency towards increased lattice constants was found [13,14], but this does not lead to a systematic improvement over the LDA. Relatively little is known about the effect of the GGC on predictions of crystalline phase stability. For the tetravalent metals Si and Ge it has been shown [15] that the GGC lead to improved predictions for the critical pressure where the transition from the four-coordinated semiconducting phase to the six-coordinated metallic phase occurs. On the other hand, it was found that the GGC do not improve the prediction of the relative stability of the layered graphitic versus the cubic diamond phase in carbon [16]. An interesting case, studied in some detail, is offered by the helical phases of Se and Te [17–19]. The equilibrium structures of these elements may be considered as arising from a Peierls distortion of the six-coordinated simple cubic structure: the two-thirds

0953-8984/95/193683+10$19.50

filled p band is unstable against a trimerization of the lattice, leading to the formation of two strong intra-chain and four weak inter-chain bonds [20]. LDA calculations [21] exaggerate the strength of the weak bonds, leading to a structure that is much more isotropic than is observed experimentally. Incorporation of the GGC greatly improves the prediction of the crystal structure and the cohesive properties of Se, but overcorrects the LDA error in the case of Te [18]. An important point to note is that the main effect of the GGC is to add an isotropic contribution to the internal pressure of the system (favouring expansion), whereas at constant volume the electronic structure and bonding properties are almost unchanged. In the present work we extend our studies of the effect of the GGC on crystal-structure predictions to the pentavalent elements As and Sb, whose zero-pressure structures result again from a Peierls distortion of the simple cubic lattice.

2. Theory

We have performed *ab initio* pseudopotential calculations of the electronic structure and total energies of As and Sb within the LDA and, in addition, incorporated GGC in the Perdew–Wang (PW) [5] and Perdew–Becke (PB) [6, 7] formulations. The calculations were performed using the VAMP (Vienna *ab initio* molecular-dynamics program) code [22, 23]. VAMP performs a variational solution of the Kohn–Sham equations within the LDA (we use the Ceperley–Alder exchange-correlation functional as parametrized by Perdew and Zunger [24]) or within the LDA + GGC on the basis of a preconditioned band-by-band conjugate-gradient approach. The equilibrium atomic structure is determined via a static or dynamic optimization of the atomic coordinates and of the cell geometry using Hellmann–Feynman forces and macroscopic stresses, via quasi-Newton and molecular dynamics algorithms, respectively. The electron–ion interaction is described by optimized ultra-soft pseudopotentials [25, 26] which ensure rapid plane-wave convergence. In each case we have used the GGC consistently, i.e. for the construction of the pseudopotential as well as for the bulk calculations. We noticed that in some cases a non-self-consistent treatment of the GGC, i.e. using them only in the valence-electron exchange-correlation functional, can lead to better results. For As and Sb we used a cut-off of $E_c = 150\,\text{eV}$. Even with a reduced cut-off of $E_c = 120\,\text{eV}$ the equilibrium structural parameters remain unchanged. The calculations were performed with a grid of $10 \times 10 \times 10$ special points (corresponding to $110\boldsymbol{k}$ points in the irreducible part of the Brillouin zone). We used a finite-temperature version of the LDA, with the fractional occupation of the eigenstates approximated by a Gaussian broadening of the one-electron energies with $\sigma = 0.1\,\text{eV}$, and the corresponding expression for the electronic entropy [18]. For the calculation of the structural energy differences, the internal energy E has been extrapolated to $\sigma \to 0$. For further technical details we refer the interested reader to [18, 23].

3. Results

The A7 crystal structure of arsenic and antimony may be described as distorted simple cubic (SC), in which there is an internal displacement of the two face-centred-cubic sublattices along the [111] direction [27]. The resulting structure has trigonal symmetry and there are two degrees of freedom in addition to the volume. One is the internal parameter u defining the relative position of the two sublattices (the displacement vector is $\boldsymbol{d} = 2u(111)/\sqrt{3}$), with $u = \frac{1}{4}$ in the SC limit and $u < \frac{1}{4}$ in the A7 lattice. The second parameter is the axial

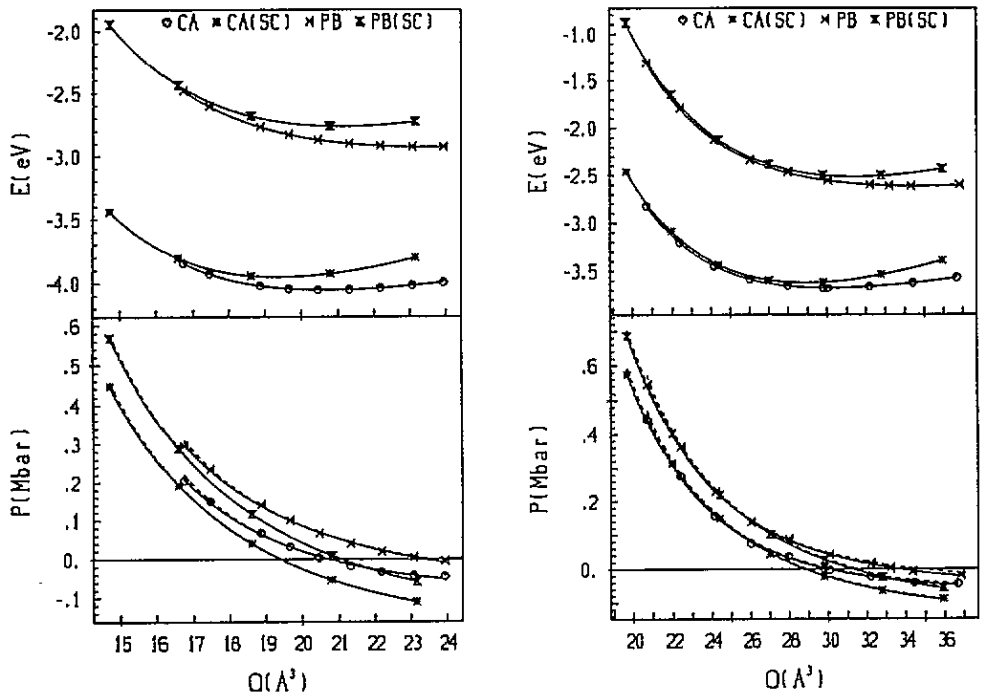

Figure 1. Energy E and pressure p in the trigonal A7 and simple cubic structures of As, calculated in the LDA with the Ceperley–Alder CA parametrization of the exchange-correlation functional and the LDA + GGC(PB) approximation. The symbols mark the calculated points, the full curves the Murnaghan fits to energies and pressures, respectively.

ratio c/a of the hexagonal cell. In the cubic limit, $c/a = \sqrt{6}$ and it is larger for the distorted structures. The distortion from cubic symmetry is caused by the half-filled p band, which makes the SC lattice unstable against a Peierls distortion [20].

3.1. Equilibrium properties

Our results for the calculated equilibrium structures and cohesive properties are compiled in table 1 and figure 1. The equilibrium structure has been determined by simultaneous optimization of the parameters of the unit cell and of the internal structural parameter u, performing the necessary corrections for the Pulay stresses. To obtain information on the change of the structure under pressure, and to obtain the bulk modulus, we have in addition performed a series of calculations at fixed volume and optimized the axial ratio c/a and the parameter u. The energies and pressures resulting from these calculations were fitted by a Murnaghan equation of state [28]. The minimum determined from the Murnaghan fit agrees well with that obtained by direct relaxation of the atomic volume.

For As, the LDA result for the equilibrium volume, structure and bulk modulus agrees well with previous LDA calculations [29–31]. Compared with experiment, the atomic volume is slightly too small, the bulk modulus is overestimated, and the relaxed structural parameters are somewhat closer to the cubic limit than in the experimental structure. This indicates that, as for the chalcogenide elements, the calculated Peierls distortion is slightly too small. The somewhat larger equilibrium volume resulting from linearized augmented plane-wave

Table 1. Calculated equilibrium structure (atomic volume Ω, axial ratio c/a, internal structural parameter u, ratio d_2/d_1 of intraplanar and interplanar distances, bond angle θ, energy difference ΔE relative to the SC phase, cohesive energy E and bulk modulus B) of trigonal As and Sb compared with experiment.

	Ω (Å^3)	c/a	u	d_2/d_1	θ (deg)	ΔE (eV)	E (eV)	B (kbar)
As								
LDA–CA[a]	20.70	2.67	0.230	1.19	96.7	0.10	4.05	0.52
PB[b]	23.45	2.92	0.225	1.27	96.6	0.16	2.92	0.36
PW[c]	27.49	2.95	0.224	1.30	96.7			
PP[d]	20.95	2.67	0.230	1.19	96.7	0.12		0.43
LAPW[e]	21.80	2.69	0.229	1.21	96.6	0.07	3.78	(0.77)
Exp.[g]	21.52	2.81	0.227	1.24	96.6			
Exp.[h]	21.30	2.78	0.228	1.23	96.4		2.96	0.38
Sb								
LDA–CA[a]	30.14	2.48	0.233	1.13	97.5	0.06	3.68	0.37
PB[b]	33.34	2.67	0.230	1.18	96.6	0.09	2.60	0.22
PW[c]	34.22	2.88	0.229	1.24	96.9			
PP[f]		2.60	0.235	1.14	95.0			
Exp.[g]	30.21	2.62	0.233	1.16	95.8			0.41

[a] LDA (Ceperley–Alder functional) present work.
[b] LDA + Perdew–Becke GGC present work.
[c] LDA + Perdew–Wang GGC present work.
[d] PP–LDA calculation (Ceperley–Alder functional) [29].
[e] LAPW–LDA (Wigner exchange functional) calculation [31]. The value for the bulk modulus is not very accurate, because the structural parameters have not been relaxed as a function of the atomic volume.
[f] PP–LDA (Wigner exchange functional) calculation [32].
[g] Exp. [33].
[h] Exp. [34–36].

(LAPW) calculations [31] (performed in the muffin-tin approximation to the potential) is a consequence of the use of the Wigner exchange functional, which always yields lower densities than the Ceperley–Alder functional used in pseudopotential calculations. The calculated energy differences relative to the SC structure is in good agreement with the pseudopotential calculation of Needs and co-workers [29,30], but larger than the LAPW result. That there should be a difference in the structural energies calculated using the PP and LAPW methods is not surprising: in the A7 structure all the strong bonds are oriented to one side of the atom, and the weak bonds to the other side. In the muffin-tin approximation, this anisotropy in the charge distribution is smeared out due to the spherical averaging. In the previous PP calculations, the structural energy difference turned out to be strongly dependent on convergence with respect to the plane-wave cut-off and to the k-point sampling. In our approach these problems are solved by the use of ultrasoft potentials and a very fine integration mesh. Under pressure, the Peierls distortion and the energy difference relative to the SC structure decrease, but the structure remains cubic up to the smallest atomic volume ($\Omega = 17$ Å^3) considered in the calculations. This again is in contrast to the LAPW result, predicting an A7 $\rightarrow$ SC transition under moderate compression. The prediction of a pressure-induced phase transition by the LAPW calculations may result from the fact that the parameters u and c/a were not allowed to change under pressure. Hence the calculation does not consider the lowest-energy A7 structure.

Inclusion of the GGC improves the results for the binding energy and the bulk modulus; for the equilibrium atomic volume and structure the PB–GGC overshoots, and this is even

more pronounced when the PW form of the GGC is used. The stabilization of the Peierls distortion by the GGC (ΔE relative to the SC structure increases from 0.1 eV atom^{-1} to 0.16 eV atom^{-1}; see table 1) confirms the result obtained for the chalcogenide elements.

For Sb, the LDA result for the atomic volume and bulk modulus is in good agreement with experiment; for the crystal structure the Peierls distortion is slightly underestimated. In this case, the GGC definitely overcorrect the good LDA results, and this effect is larger for the PW form than for the PB form.

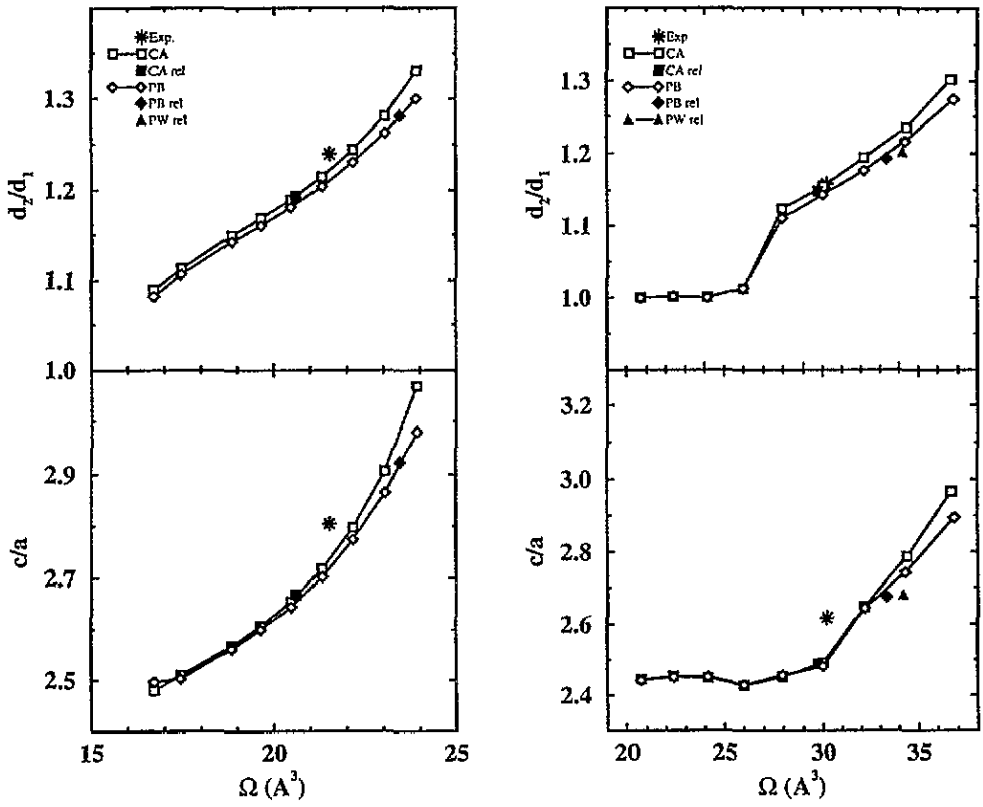

Figure 2. Variation of the ratio d_2/d_1 of the lengths d_1 and d_2 of intralayer and interlayer distances and of the axial ratio c/a as a function of the atomic volume for trigonal As (*a*) and Sb (*b*). Squares: LDA in the Ceperley–Alder (CA) parametrization; diamonds: LDA + GGC(PB); triangles: LDA + GGC(PW). The open symbols represent the results obtained at fixed volume. The full symbols represent the results of a simultaneous relaxation of structure and volume. The stars represent experiment.

3.2. Phase transition under pressure

Figure 2 shows the variation of the axial ratio and of the ratio of the second- and first-neighbour distances (i.e. the lengths of the weak and strong bonds) with the atomic volume. Independent of the treatment of exchange-correlation effects, the structure becomes more isotropic under compression. However, *at fixed atomic volume the inclusion of the GGC does*

not change the crystal structure, confirming the result we had obtained earlier for the case of the chalcogenides. Hence the main effect of the GGC is to add an isotropic contribution to the internal pressure, favouring expansion. That the effect of the GGC is isotropic can be understood on the basis of a result presented by Juan and Kaxiras [12], who analysed the difference of the LDA and LDA + GGC exchange-correlation energy functionals and potentials for the case of Si. It was shown that the most important differences occur in the core region; this is not surprising, since the density varies significantly in this region. Even in the pseudopotential approximation, where the pseudo-electron densities in the core region are small, the gradients are still large. Hence the effect of the GGC is mainly isotropic.

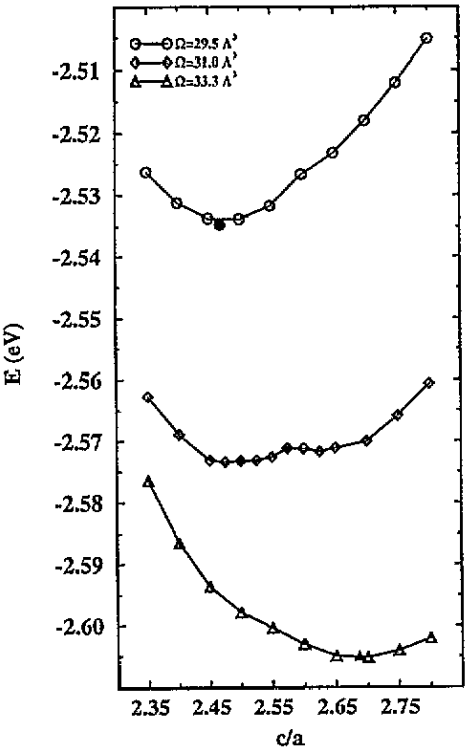

Figure 3. Variation of the binding energy of Sb as a function of the axial ratio c/a at three fixed atomic volumes close to the A7–SC phase transition. The symbols mark the relaxed values (with respect to u at fixed c/a) (open symbols) and with respect to u and c/a simultaneously (full symbols); the lines are simply there as a guide to the eye.

A pressure-induced A7–SC phase transition has been reported [37] for Sb (but not for As), but more recent experiments have claimed that such a transition occurs only under non-hydrostatic pressure [38]. Figure 1 shows that for Sb the Peierls distortion and the structural energy difference A7–SC decrease rapidly under pressure and vanish for $\Omega < 26\,\text{Å}^3$. For smaller atomic volumes the relaxation of the structural parameters leads to a SC structure; the Peierls-distorted structure is unstable. It is interesting that the axial ratio converges to $c/a = \sqrt{6}$ before the parameter u describing the relative displacement of the two sublattices converges to $u = \frac{1}{4}$ (see figure 2). Figure 3 shows the variation of the energy with the axial ratio at three different atomic volumes ($\Omega = 33.3\,\text{Å}^3$, $31.0\,\text{Å}^3$ and $29.5\,\text{Å}^3$). At $\Omega = 33.3\,\text{Å}^3$, the energy has a single minimum at an axial ratio of $c/a = 2.69$, at $\Omega = 31.0\,\text{Å}^3$ the energy has two minima at $c/a = 2.57$ and $c/a = \sqrt{6}$, and at $\Omega = 29.5\,\text{Å}^3$ a single minimum at $c/a \sim \sqrt{6}$. The corresponding equilibrium values of u at the optimal c/a are $u = 0.229$, 0.232 and 0.236, respectively. They vary only little with c/a. The simple cubic limit

of $u = \frac{1}{4}$ is reached only at $\Omega = 26.0\,\text{Å}^3$. There is no difference between the LDA and LDA + GGC results (see figure 2). The transition pressure is estimated from the condition that the pressure be equal in both phases, with the result $p_c \sim 40$ kbar (LDA) and $p_c \sim 70$ kbar (LDA + GGC(PB)). The LDA + GGC value agrees with the transition pressure reported by Kabalkina and co-workers [37]. However, a quantitative estimate is difficult because the transition is almost continuous.

An indication that the transition is first order, as found in experiment [37], can be derived only from the abrupt variation of u and d_2/d_1 between $\Omega = 27.9\,\text{Å}^3$ and $\Omega = 26.0\,\text{Å}^3$. Experimentally, the change of volume at the transition has been estimated to be 0.5%. To derive a theoretical estimate for the discontinuity of the volume, it would be necessary to perform the calculations of ΔE on a very fine mesh of atomic volumes. At these compressions, c/a has already assumed the cubic value and the transition occurs via a change of u only. That in stabilizing the A7 structure the sublattice displacements dominate over the rhombohedral shear agrees with the pseudopotential calculations of Chang and Cohen [32], who predicted a nearly continuous phase transition driven by a longitudinal acoustic R-point phonon of the SC phase. The phonon frequency is calculated to be imaginary for $\Omega/\Omega_{equ} \geqslant 0.86$. The reduced volume for the transition agrees with our result; no pressure has been calculated.

For As, an A7–SC phase transition is not predicted for pressures smaller than 200 kbar (LDA) and 300 kbar (LDA + GGC(PB)), i.e. at pressures that are much larger than the A7–SC transition pressures measured for Sb and P ($p_c = 70$ kbar and 110 kbar, respectively [37, 39]. At these pressures, the differences between the A7 and SC structures are already quite small ($d_2/d_1 \sim 1.08$, $c/a - \sqrt{6} \sim 0.04$) and an almost continuous transition should occur at slightly larger pressure. The increased stability of the A7 phase for As compared to Sb and P may be attributed to the stronger non-locality of the electron–ion potential: in As the 4s electrons partially penetrate the 3d core and hence experience a more attractive potential than the 4p electrons. This results in a larger s–p separation and a reduced s–p hybridization in As, which contributes to a stabilization of the Peierls distortion arising from the formation of covalent (ppσ) bonds.

3.3. Electronic structure

Figure 4 shows the results for the electronic densities of states (DOS) of Sb at the equilibrium volumes of the LDA, LDA + GGC(PB) and LDA + GGC(PW) calculations and close to the A7–SC phase transition. The band structure is characterized by an s-band below ~ 5.5 eV binding energy and a p band close to the Fermi level. Both bands display the characteristic Peierls gap in the middle of the band, coincident with the bonding–antibonding splitting. The Fermi energy falls into the Peierls gap of the p band. The effect of the GGC is again mainly a volume effect: it reduces the band width of the Peierls-split subbands and slightly increases the internal s–p gap, but not the Peierls gap at the Fermi level. At fixed volume the DOS is virtually unchanged. The calculated DOS is in very good agreement with the earlier calculations [29–31] (apart from a somewhat lower DOS in the pseudogap at the Fermi level, which may be a consequence of the finer k-space sampling in our calculations) and for both As and Sb with the measured photoemission spectra [40, 41].

Under pressure the widths of the subbands gradually increase, but the Peierls gaps do not disappear until the phase transformation has been completed. Figure 4(b) shows the density of states close to the phase transition: at a volume where the A7 structure with $c/a \neq \sqrt{6}$ and $u < \frac{1}{4}$ is marginally stable, at a volume where $c/a = \sqrt{6}$ but $u < \frac{1}{4}$, and in the simple cubic phase. Even in the SC high-pressure phase at $\Omega = 26.0\,\text{Å}^3$, a bonding–antibonding pseudogap (minimum in the DOS) subsists in the middle of both the s and the

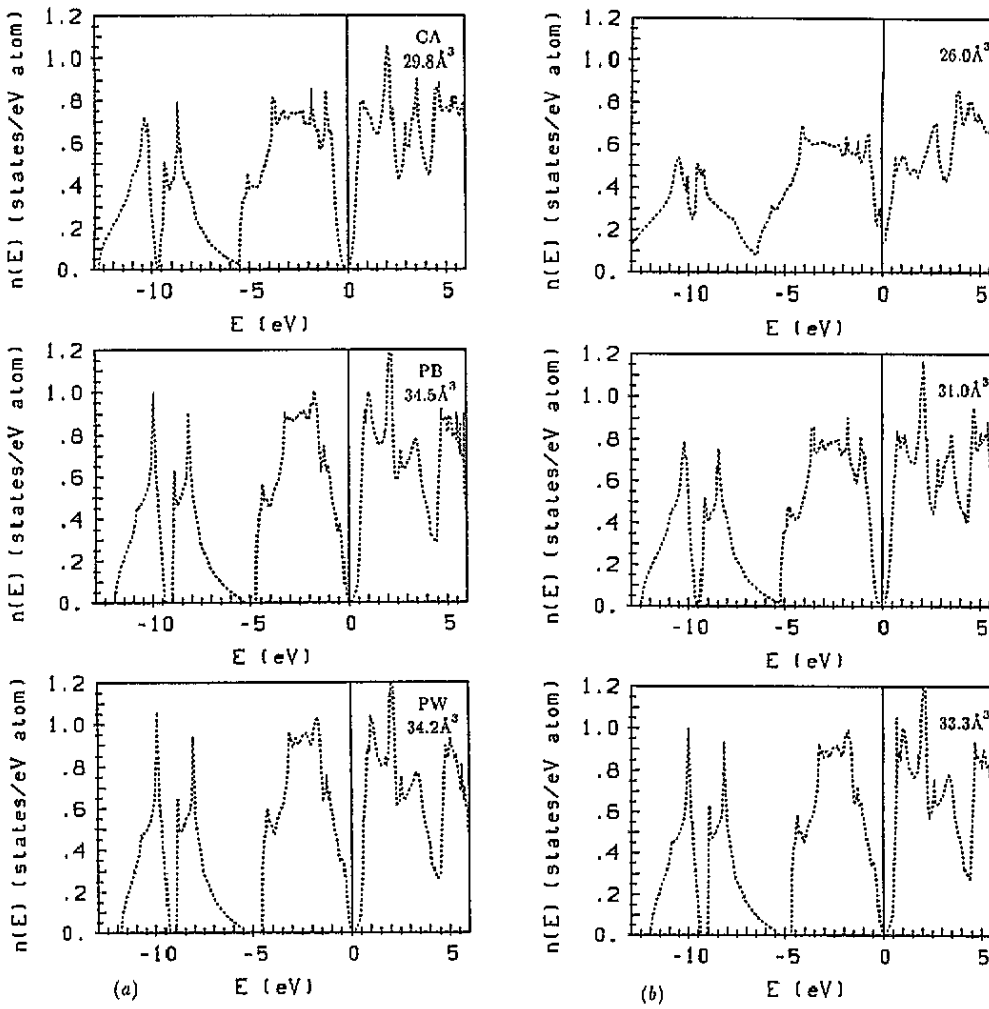

Figure 4. Electronic densities of states of Sb for the equilibrium structures obtained in the LDA(CA) and LDA + GGC(PB PW) approximations (*a*) and close to the A7–SC phase transition in relaxed states shown in figure 3: the compressed A7 phase, the intermediate state and the SC high-pressure phase (calculated in the LDA + GGC(PB) approximation).

p band. This shows that as the structural phase transition the semimetal–metal transition is quasi-continuous.

4. Conclusions

Our investigations of the influence of GGC on the crystal structures of the low-symmetry phases of the pnictide and chalcogenide elements lead to concordant results: at fixed volume, the inclusion of GGC changes neither the predicted atomic structure nor the electronic band structure, and the changes of the crystal structures and band structures as a function of volume are identical with and without GGC. The GGC, however, influence the equilibrium atomic volume by adding an isotropic contribution to the internal pressures, favouring

expansion. For Se, this leads to an important improvement over the LDA; for As and Te the GGC overcorrect the LDA error, with the LDA and LDA + GGC results about equidistant from experiment; for Sb the LDA is already a good approximation and the agreement with experiment is reduced by adding GGC. The predicted transition pressure for the A7–SC phase transition, however, is more realistic *with* than without the GGC. The overshoot effect can be reduced by using the GGC only for the solid state, but not for the construction of the pseudopotential; however, we do not consider this to be a justifiable procedure.

It is still very difficult to see a consistent trend in the applications of GGC to the calculations of cohesive and structural properties. Körling and Häglund [14] found that for the 3d transition metals the GGC lead to important improvements, but for the 4d and 5d metals the GGC definitely overshoot. For the s, p-bonded elements the situation is even more confusing: even for the simple case of face-centred cubic Al, there are conflicting reports that the addition of GGC either increases [12] the lattice constant by 8% or lowers it by 0.5% [10]. There are also conflicting reports as to whether the GGC change [10] the prediction for the gap in semiconductors or do not affect it at all [11]. The present study represents an attempt to bring some systematics into these investigations: we find that the GGC become less reliable with increasing atomic number and with increasing isotropy of the crystal structure. The first point would seem to agree with the conclusion drawn from the study of transition metals, but evidently much further work is needed.

Acknowledgments

This work has been supported by the Austrian Science Foundation under project no. P10445-PHYS. GK has been supported by Siemens–Nixdorf Austria within the contract of cooperation with the Technische Universität Wien.

References

[1] Hohenberg P and Kohn W 1964 *Phys. Rev.* **136** B864
Kohn W and Sham L J 1965 *Phys. Rev.* **140** A1133
Kohn W 1985 *Highlights of Condensed Matter Theory* ed M P Tosi, M Fumi and F Bassani (Amsterdam: North-Holland)
[2] Jones R O and Gunnarsson O 1989 *Rev. Mod. Phys.* **61** 689
[3] Ihm J 1988 *Rep. Prog. Phys.* **51** 105
[4] Pickett W E 1989 *Comput. Phys. Rep.* **9** 115
[5] Perdew J P and Wang Y 1986 *Phys. Rev.* B **33** 8800
[6] Perdew J P 1986 *Phys. Rev.* B **33** 8822
[7] Becke A D 1988 *Phys. Rev.* A **38** 3038
[8] Ma S K and Brueckner K A 1968 *Phys. Rev.* **165** 18
[9] Langreth D C and Mehl M J 1981 *Phys. Rev. Lett.* **47** 446
[10] Kong X J, Chan C T, Ho K M and Ye Y Y 1990 *Phys. Rev.* B **42** 9357
[11] Ortiz G 1992 *Phys. Rev.* B **45** 11 328
[12] Juan Yu-Min and Kaxiras E 1993 *Phys. Rev.* B **48** 14 994
[13] Garcia A, Elsässer C, Zhu J, Louie S G and Cohen M L 1992 *Phys. Rev.* B **46** 9829
[14] Körling M and Häglund J 1992 *Phys. Rev.* B **45** 13 293
[15] Scheffler M 1995 to be published
[16] Furthmüller J, Hafner J and Kresse G 1994 *Phys. Rev.* B **50** 15 506
[17] Akbarzadeh H, Clark S J and Ackland G J 1993 *J. Phys.: Condens. Matter* **5** 8065
[18] Kresse G, Furthmüller J and Hafner J 1994 *Phys. Rev.* B **50** 13 181
[19] Dal Corso A and Resta R 1994 *Phys. Rev.* B **50** 4327
[20] Littlewood P B 1983 *Crit. Rev. Solid State Mat. Sci.* **11** 229

[21] Vanderbilt D and Joannopoulos J D 1983 *Phys. Rev.* B **27** 6296
[22] Kresse G and Hafner J 1993 *Phys. Rev.* B **47** 585; *Phys. Rev.* B **48** 13 115
[23] Kresse G and Hafner J 1994 *Phys. Rev.* B **49** 14 251
[24] Perdew J P and Zunger A 1981 *Phys. Rev.* B **23** 5048
[25] Vanderbilt D 1990 *Phys. Rev.* B **41** 1227
[26] Kresse G and Hafner J 1994 *J. Phys.: Condens. Matter* **6** 5825
[27] Young D A 1992 *The Phase Diagrams of the Elements* (New York: Wiley)
[28] Wallace D C 1972 *Thermodynamics of Crystals* (New York: Wiley) p 51
[29] Needs R J, Martin R M and Nielsen O H 1986 *Phys.Rev.* B **33** 3778
[30] Needs R J, Martin R M and Nielsen O H 1987 *Phys. Rev.* B **35** 9851
[31] Mattheis L F, Hamann D R and Weber W 1986 *Phys. Rev.* B **34** 2190
[32] Chang K J and Cohen M L 1986 *Phys. Rev.* B **33** 7371
[33] Villars P and Calvert L D 1990 *Pearson's Handbook of Crystallographic Data for Intermetallic Phases* (Metals Park: Am. Soc. Metals)
[34] Schiferl D and Barrett C S 1969 *J. Appl. Cryst.* **2** 30
[35] Kittel C 1976 *Introduction to Solid State Physics* 5th edn (New York: Wiley)
[36] Morosin B and Schirber J E 1972 *Solid State Commun.* **10** 249
[37] Kabalkina S S and Mylov V P 1964 *Sov. Phys. Dokl.* **8** 917
Kolobyanina T N, Kabalkina S S, Vereshchagin L F and Fedina L V 1969 *Sov. Phys.-JETP* **28** 88
[38] Schiferl D, Cromer D T and Jamieson J C 1981 *Acta Cryst.* B **37** 807
[39] Kikegawa T and Iwasaki H 1983 *Acta Crystallogr.* B **39** 158
[40] Ley L, Pollak R A, Kowalczyk S P, McFeely F R and Shirley D A 1973 *Phys. Rev.* B **8** 641
[41] Tokailin H, Takahashi T, Sagawa T and Shindo K 1984 *Phys. Rev.* B **30** 1765